Published online 26 December 2016 *Nucleic Acids Research, 2017, Vol. 45, No. 3* ***1041–1048***
doi: 10.1093/nar/gkw1294

Salt-mediated two-site ligand binding by the cocaine-binding aptamer

Miguel A.D. Neves†, Sladjana Slavkovic†, Zachary R. Churcher and Philip E. Johnson*

Department of Chemistry and Centre for Research on Biomolecular Interactions, York University, Toronto, Ontario M3J 1P3, Canada

Received October 30, 2016; Revised December 10, 2016; Editorial Decision December 12, 2016; Accepted December 13, 2016

ABSTRACT

Multisite ligand binding by proteins is commonly utilized in the regulation of biological systems and exploited in a range of biochemical technologies. Aptamers, although widely utilized in many rationally designed biochemical systems, are rarely capable of multisite ligand binding. The cocaine-binding aptamer is often used for studying and developing sensor and aptamer-based technologies. Here, we use isothermal titration calorimetry (ITC) and NMR spectroscopy to demonstrate that the cocaine-binding aptamer switches from one-site to two-site ligand binding, dependent on NaCl concentration. The high-affinity site functions at all buffer conditions studied, the low-affinity site only at low NaCl concentrations. ITC experiments show the two ligand-binding sites operate independently of one another with different affinities and enthalpies. NMR spectroscopy shows the second binding site is located in stem 2 near the three-way junction. This ability to control ligand binding at the second site by adjusting the concentration of NaCl is rare among aptamers and may prove a useful in biotechnology applications. This work also demonstrates that *in vitro* selected biomolecules can have functions as complex as those found in nature.

INTRODUCTION

Controlling biomolecular function is an important area of chemical biology. In nature, there are many ways in which the activity of proteins and nucleic acids are controlled including genetic control, allosteric effectors and covalent modification. For rationally designed biosystems, having control over the function of molecules is a desired, but difficult to achieve capability. Aptamers have been used in a modular manner to control nucleic acid-based enzymes and molecular devices (1,2) typically in a fashion where aptamer binding leads to a structural change that activates an associated enzyme or receptor molecule. However, more subtle examples of biomolecular control where, for example, changes in solution composition leading to a change in activity or function, are rare or not currently known.

The cocaine-binding aptamer, originally reported in the early 2000s, has become a model system routinely implemented in the study and development of small molecule sensing and aptamer-based technologies (3–16). The widespread use of the cocaine-binding aptamer continues despite the fact the aptamer was revealed to bind quinine and quinine analogs with up to 50 fold higher affinity than cocaine, the target that the aptamer was initially selected to bind (17–20). The reason for the continued utilization of the cocaine-binding aptamer likely lies in the ability to engineer into the aptamer a structure switching binding mechanism. The secondary structure of the MN4 aptamer (Figure 1) is pre-formed in the absence of ligand, and upon binding its target there is no observable change in the secondary structure (21). However, if the length of stem one is shortened to three base pairs, such as for MN19 (Figure 1), the aptamer is loosely structured in the absence of target and upon binding the secondary structure rigidifies in a ligand-induced folding process (4,21). This ligand-induced folding mechanism is retained with quinine binding and when the sequence is altered to allow for binding of the steroid deoxycholic acid (DCA) (18,22). The cocaine-binding aptamer has also been shown to function when separated into two strands, referred to as a split-aptamer (3,13,23). The majority of published cocaine-aptamer based technologies rely on the use of the structure-switching or split-aptamer sequence variants.

Multisite ligand binding is commonly observed in proteins but less frequently observed in functional nucleic acids such as aptamers and riboswitches. Multisite ligand binding can be independent or cooperative, with both positive and negative cooperativity possible. A classic example of multisite binding occurring in nature is the binding of oxygen to hemoglobin, which occurs in a positively cooperative man-

*To whom correspondence should be addressed. Tel: +1 416 736 2100 (Ext 33119); Email: pjohnson@yorku.ca
† The authors wish it to be known that, in their opinion, the first 2 authors should be regarded as joint First Authors.
Present Address: Miguel A. D. Neves, Department of Laboratory Medicine, Keenan Research Centre for Biomedical Science, St. Michael's Hospital, Toronto, Ontario, Canada, M5B 1W8.

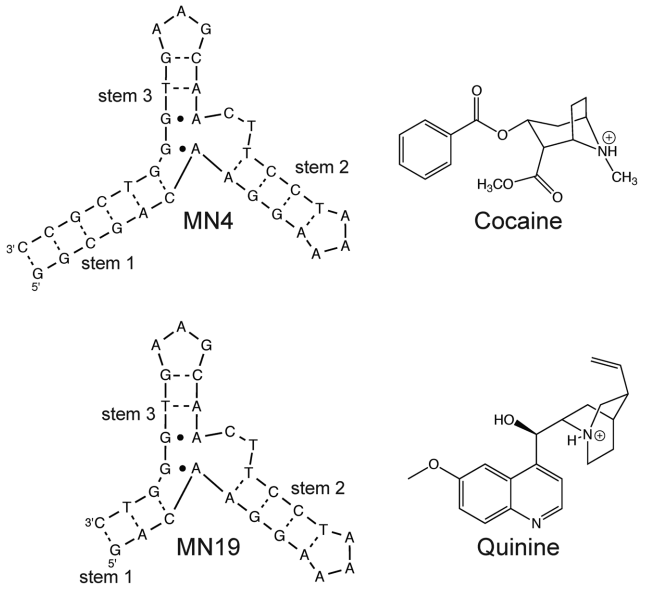

Figure 1. Secondary structure of the MN4 and MN19 cocaine-binding aptamers and chemical structures of the cocaine and quinine ligands. Dashes between nucleotides indicate Watson–Crick base pairs while dots indicate non-Watson–Crick base pairs.

ner. Despite the prevalence of multisite ligand binding in proteins and enzymes, it is rare to find examples of multisite binding among functional nucleic acids. One example is the tetrahydrofolate (THF) riboswitch that binds two ligands in a cooperative manner (24). Another example is for the ATP binding DNA aptamer that binds two ATP molecules at separate sites (25,26). An RNA aptamer for neomycin B was demonstrated to bind one neomycin B ligand at a high affinity site and have two additional low affinity sites at which binding can be disrupted by addition of NaCl (27). In a slightly different example, the activity of a ribozyme was controlled by engineering an FMN and a theophylline aptamer into the structure of the hammerhead ribozyme to produce a ribozyme whose activity was controlled by the binding of these two different ligands (28).

In this study, we show that the cocaine-binding aptamer binds two molecules of its ligand in buffer conditions of low NaCl concentration. Additionally, we demonstrate that binding at the second site can be controlled by varying the NaCl concentration of the buffer. Ligand binding at the first site continues to occur in all buffer conditions studied. Salt-controlled binding could be utilized in applications employing this aptamer where an increased affinity or aptamer rigidity could be beneficial, such as in sensing, by simply changing the NaCl concentration of the buffer.

MATERIALS AND METHODS

Materials

All aptamer samples (Figure 1) were obtained from Integrated DNA Technologies (IDT). DNA samples were dissolved in distilled deionized H_2O (ddH_2O) and then exchanged three times using a 3 kDa molecular weight cutoff concentrator with sterilized 1 M NaCl followed by three exchanges into ddH_2O. Aptamer concentrations were determined by UV absorbance spectroscopy using the extinction coefficients supplied by the manufacturer. Cocaine hydrochloride and quinine hemisulfate monohydrate were obtained from Sigma-Aldrich. The pH of Tris buffers were adjusted to 7.4 at room temperature and not adjusted for temperature effects.

Isothermal titration calorimetry

The ITC experiments were performed using a MicroCal VP-ITC instrument. Samples were degassed prior to use with a MicroCal ThermoVac unit. All experiments were acquired at 15°C and corrected for the heat of dilution of the titrant. All titrations were performed with the aptamer in the cell and the ligand in the syringe. All aptamer samples were heated in a boiling water bath for 3 min and cooled in an ice bath preceding ITC experiments to allow the aptamer to anneal. Binding experiments consisted of 35 successive 8 μl injections spaced every 300 s where the first injection was 10 μl to account for diffusion from the syringe into the cell during equilibration. This initial injection was not used in fitting the data. For titrations of MN4 at aptamer concentrations of 56, 80 and 130 μM, a first injection of 30 μl was used.

Cocaine binding experiments were performed with MN4 aptamer solutions of 56, 80 and 130 μM using ligand concentrations of 0.7, 1.4 and 2.8 mM, respectively, in a buffer of 20 mM Tris (pH 7.4) with either 0 mM or 140 mM NaCl. Quinine binding experiments with varying *c*-values ($c = [\text{aptamer}]/K_d$) were performed with MN4 aptamer solutions of 11, 19, 42, 56, 80 and 130 μM using ligand concentrations of 0.156 to 3.01 mM in 5 mM Tris (pH 7.4). MN19 quinine binding experiments were performed with concentrations of 200 μM and 3.12 mM aptamer and ligand, respectively, in 20 mM Tris (pH 7.4). Quinine binding experiments with varying NaCl concentrations were performed with MN4 aptamer solutions of 20 μM using a ligand concentration of 0.312 mM in 20 mM Tris (pH 7.4) with NaCl concentrations of 0, 25, 50, 75 and 140 mM. In all experiments, cocaine and quinine solutions were prepared in the same buffer as the aptamer.

Data fitting

One-site ITC data were fit to a one-set-of-sites binding model using the manufacturer-provided data-fitting package within Origin 7. The data for two-site binding were fit to a two-independent sites binding model as developed by Freiburger *et al.* (29) The fitting of the two-site binding data was performed using the Matlab 14 software package.

NMR spectroscopy

NMR experiments on aptamer samples were performed using either a 600 MHz Bruker Avance spectrometer equipped with a ^{1}H-^{13}C-^{15}N triple-resonance probe or a 700 MHz Bruker Avance III spectrometer equipped with ^{1}H-^{13}C-^{15}N triple-resonance cryoprobe. All NMR spectra were acquired in $^{1}H_2O/^{2}H_2O$ (90%/10%) at 5°C. Water suppression was achieved through the use of the WATERGATE se-

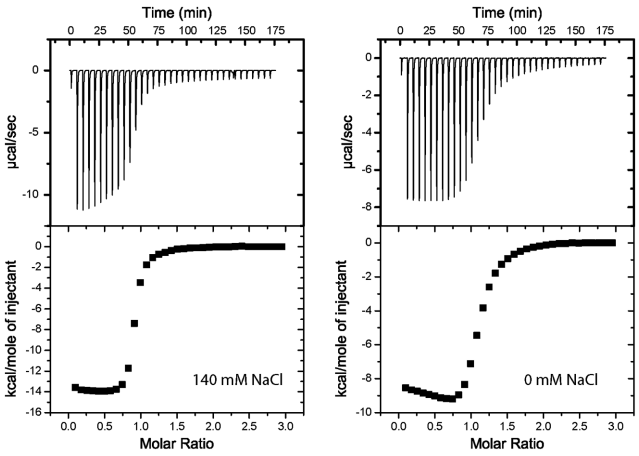

Figure 2. Demonstration of two-site binding by the cocaine-binding aptamer using ITC. Shown are the titrations of cocaine into a solution of the MN4 aptamer with buffer conditions of (**Left**) 140 mM NaCl and (**Right**) 0 mM NaCl. The non-sigmoidal nature of the binding curve in 0 mM NaCl indicates that more than one binding event is occurring. On top is the titration data showing the heat resulting from each injection of cocaine into an aptamer solution. On bottom are the integrated heats after correcting for the heat of dilution. Both binding experiments were performed at 15°C and also contained 20 mM Tris (pH 7.4).

quence or excitation sculpting (30,31). Aptamer concentrations for NMR studies varied from 0.2 to 1.8 mM.

RESULTS AND DISCUSSION

Salt-controlled two-site binding of cocaine

The ability of the cocaine-binding aptamer to bind more than one ligand is clearly demonstrated by the shape of the ITC thermogram when cocaine is titrated into a solution of aptamer in the absence of NaCl (Figure 2). The non-sigmoidal-shaped binding curve we observe when MN4 binds cocaine with no NaCl present contrasts sharply with the binding thermogram for MN4 in the presence of 140 mM NaCl and indicates that more than one binding event is taking place. The ITC data indicates that the stoichiometry of this multi-site interaction is two-site binding as the thermogram saturates after the addition of two molar equivalents of cocaine. The dip at the start of the ITC thermogram indicates that the second (lower affinity) site is more exothermic than the first (higher affinity) site. As the second site starts to be populated the overall enthalpy becomes more negative, then, as both sites saturate the total enthalpy is progressively less negative.

This two-site binding data was then fit to a two-independent site binding model in order to determine the affinity and binding enthalpy of each of the two sites (29). A feature of this two-independent site binding model is that the ITC isotherms analyzed vary as a function of receptor concentration. Hence, the average of the fits from ITC experiments performed at three different MN4 concentrations resulted in a K_{d1} value of 1.3 ± 0.4 μM, a ΔH_1 of −10 ± 1 kcal mol^{-1}, and a $-T\Delta S_1$ of 2.5 ± 1.1 kcal mol^{-1} (high affinity site), while the low affinity site has a K_{d2} value of 16 ± 8 μM, a ΔH_2 of −20 ± 2 kcal mol^{-1}, and a $-T\Delta S_2$ of 13 ± 2 kcal mol^{-1}. The other potential binding models of identical independent and identical cooperative binding (32) were not considered as it is not possible to have two identical binding sites within the monomeric cocaine-binding aptamer. The high affinity site is slightly tighter with no added NaCl than previously reported in 140 mM NaCl (5.5 ± 0.4 μM) at the same pH value and temperature (19). This higher affinity in the absence of NaCl is consistent with electrostatic interactions playing a role in the affinity of the positively charged ligand to the polyanionic DNA (18,23) as reducing the salt concentration will decrease shielding of the charge-charge interactions, increasing the electrostatic attractions and yielding higher affinity.

Salt-mediated two-site binding of quinine

The low NaCl-dependent two-site binding phenomenon of the cocaine-binding aptamer was interrogated for quinine binding. MN4 was previously shown to bind quinine ∼50-fold tighter than cocaine (17–19). This higher affinity enables us to conveniently perform ligand binding experiments at a wide range of c-values in order to better define the independent two-site binding model using global fitting, where all c-values are fit to the same parameters simultaneously (29). ITC experiments were performed at six MN4 concentrations that ranged from 11 to 130 μM. Using global fitting, the affinity of MN4 for quinine at the high affinity site (K_{d1}) was determined to be 0.17 ± 0.07 μM, the enthalpy (ΔH_1) was found to be −10.8 ± 0.5 kcal mol^{-1} and the $-T\Delta S_1$ is 1.9 ± 0.8 kcal mol^{-1} while the low affinity site has a K_{d2} value of 1.2 ± 0.6 μM, a ΔH_2 of −26 ± 3 kcal mol^{-1} and a $-T\Delta S_2$ is 19 ± 9 kcal mol^{-1} (Figure 3). These data from the global fits agree within the error range with the average of the individual fits which are, for the high affinity site, a K_{d1} value of 0.3 ± 0.2 μM a ΔH_1 of −10.6 ± 0.9 kcal mol^{-1} and a $-T\Delta S_1$ of 1.9 ± 0.5 kcal mol^{-1} while the low affinity site has an average of the individual fits with a K_{d2} value of 3 ± 2 μM and a ΔH_2 of −31 ± 15 kcal mol^{-1} and a $-T\Delta S_2$ of 24 ± 4 kcal mol^{-1}. The K_d value for MN4 binding quinine in 140 mM NaCl is 0.20 ± 0.05 μM with a ΔH of −14 ± 1 kcal mol^{-1}.

We further investigated the effect of NaCl concentration on MN4-quinine binding by performing ITC experiments at NaCl concentrations ranging from 0 to 140 mM. Figure 4 shows the raw thermograms acquired at different concentrations of NaCl. The shapes of the thermograms clearly demonstrate the shift from two-site to one-site binding as the concentration of NaCl increases. Presumably, at higher Na^+ concentrations the cation shields electrostatic interactions between the negatively charged DNA aptamer and the positively charged quinine (or cocaine) ligand. It is likely that electrostatic interactions play a greater role in ligand binding at the low affinity site as Na^+ abolishes binding at high concentrations. This increased role of electrostatics at the low affinity site is consistent with the ITC-determined enthalpy at this site being more exothermic than at the high affinity site.

Many of the applications of the cocaine-binding aptamer rely on the structure-switching binding mechanism of a short stem 1 sequence variant. We analysed the interaction of the cocaine-binding aptamer construct MN19 (Figure 1) in order to assess a short stem 1 variant for two-site bind-

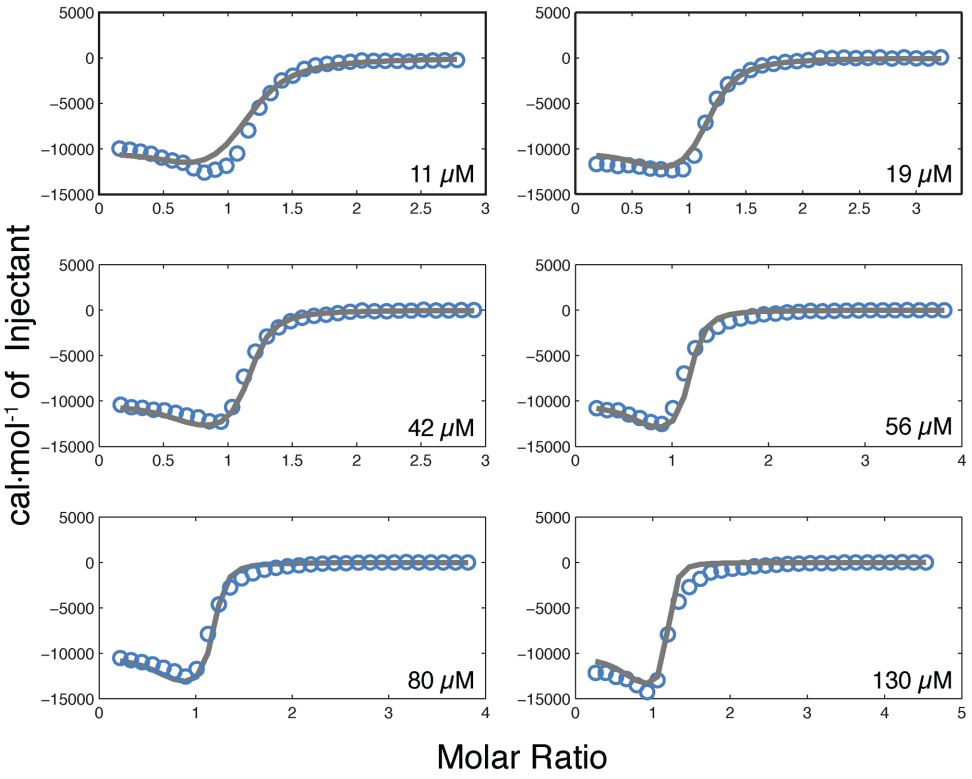

Figure 3. ITC data for MN4 binding quinine acquired at various aptamer concentrations at 0 mM NaCl. Shown in blue circles are the experimental data with the global fit of the data to an independent sites model displayed in a solid gray line.

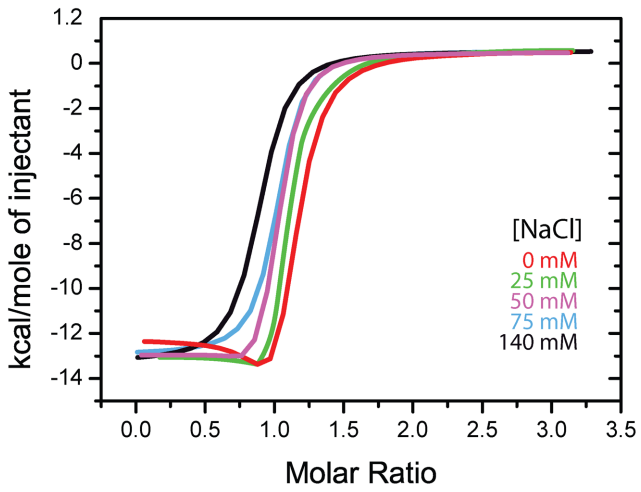

Figure 4. Ligand binding at the second site is controlled by the concentration of NaCl. Shown are the ITC data for the titration of MN4 with quinine at different NaCl concentrations. In red is data at 0 mM; green at 25 mM; purple at 50 mM; blue at 75 mM and black at 140 mM NaCl. Experiments were performed at 15°C and also contained 20 mM Tris (pH 7.4).

ing. ITC experiments were performed at both high and low NaCl concentrations and, as seen with the long stem 1 construct, MN19 binds two quinine molecules at 0 M NaCl. The affinity of MN19 for quinine in 20 mM Tris pH 7.4, 0 mM NaCl has a K_{d1} value of 0.28 ± 0.12 μM, a ΔH_1 of −8.5 ± 0.2 kcal mol^{-1} and a $-T\Delta S_1$ of −0.13 ± 0.06 kcal mol^{-1} at the high affinity site, while the low affinity site has a K_{d2} value of 4.9 ± 0.9 μM a ΔH_2 of −68 ± 42 kcal mol^{-1} and a $-T\Delta S_2$ of 61 ± 40 kcal mol^{-1} (Supplementary Figure S1). The error in ΔH_2, and consequently ΔS_2, is high as only one aptamer concentration was analysed and the '*c* value' at the second site is significantly lower than at the high affinity site. This does not distract from the main goal that is to show that MN19 behaves similarly to MN4 at low NaCl concentrations. At 140 mM NaCl, MN19 binds quinine only at a single site with an affinity of 0.38 ± 0.09 μM and a ΔH of −15.2 ± 3.2 kcal mol^{-1}. These values match within the error range with what we reported earlier for quinine binding with the same buffer conditions though at slightly different temperatures (17.5 versus 15°C) (18).

Structural analysis of two-site binding using NMR spectroscopy

In order to obtain structural insights about the location of the second (low affinity) ligand-binding site, we monitored a titration of MN4 with cocaine using NMR spectroscopy (Figure 5). Two titrations at different NaCl concentrations were performed, one at 0 M NaCl and a second at 200 mM NaCl. For the titration at 200 mM NaCl the 1D-^{1}H NMR spectrum of the imino region of the unbound aptamer is essentially identical to the MN4 spectrum we assigned and reported previously (21). Upon addition of one equivalent of cocaine we observed a number of changes in the NMR spectrum indicative of cocaine binding. In particular, G31 moves upfield and T19 appears as the most downfield imino

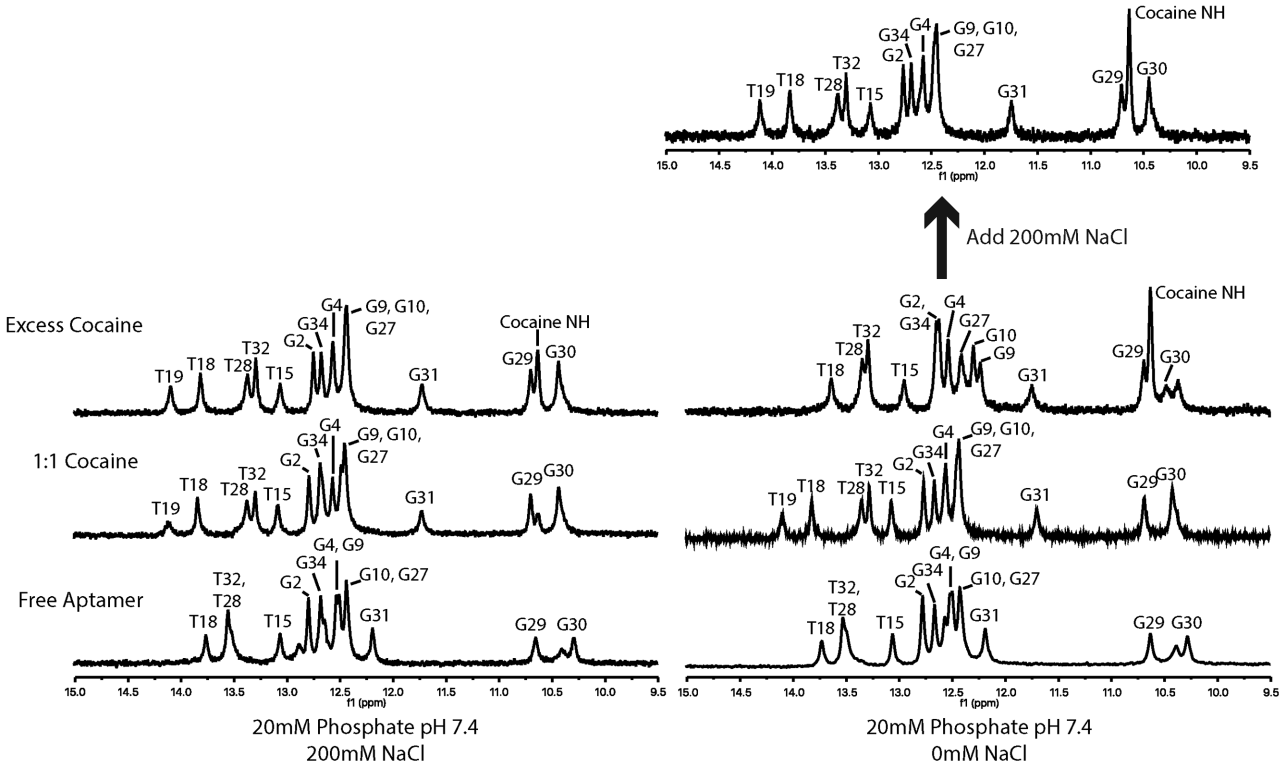

Figure 5. Cocaine binding by MN4 monitored by 1D ^{1}H-NMR. Displayed is the region of the NMR spectrum focusing on the imino resonances as a function of increasing cocaine concentration. On the left is a titration in the presence of 200 mM NaCl and no chemical shift changes are observed after the binding of 1 molar equivalent of cocaine. On the right is a titration performed with no NaCl present. Numerous resonances change chemical shift past the binding of 1 molar equivalent of cocaine. At the top right is the spectrum where NaCl, to a concentration of 200 mM, was added to the sample with excess cocaine with no NaCl (directly below it). All spectra were acquired at 5°C.

signal (Figure 5). These changes are consistent with our previously published MN4•(cocaine) spectrum (21). With the addition of cocaine past a 1:1 ratio no further changes in the 1D-^{1}H NMR imino spectrum of MN4 in 200 mM NaCl were observed. Even with a 40-fold excess of cocaine no further NMR spectral changes are observed, this is consistent with the ITC derived binding data reported above.

The NMR spectrum of MN4 in the absence of NaCl was acquired in order to see the effects of ligand binding at the low-affinity binding site. The NMR spectra of the free and 1:1 bound MN4 samples were essentially identical to that acquired in 200 mM NaCl. The only difference is in the location of the G24 imino proton in the loop of stem 3. At 0 mM NaCl with the addition of cocaine past a 1:1 ratio we see numerous changes in the spectrum indicative of cocaine binding at the low affinity binding site (Figure 5). The signals affected by binding at the low affinity site are in fast exchange on the NMR timescale. In order to saturate the low affinity site and observe the spectrum of MN4•(cocaine)$_2$, a large (40-fold) excess of ligand needed to be added (Figure 5; Supplementary Figure S2).

We assigned the imino spectrum of the MN4•(cocaine)$_2$ sample through the analysis of a 2D NOESY spectrum (Supplementary Figure S3). The assignments obtained are indicated in Figure 5. The base pairs whose imino protons shift most from the 1:1 to 2:1 cocaine-bound states are shown in the histogram in Figure 6 and are indicated in the secondary structure diagram by shades of gray. The imino protons that change chemical shift most with binding at the low affinity site are, with the exception of G2, all located in stem 2 (Figure 6). This contrasts sharply with the signals that shift most with one molecule of cocaine binding which are, in decreasing order of $\Delta\delta$, G31, T32, G30 and T28. (21) G31, which shifts most with ligand binding at the high affinity site, only shifts minimally with ligand binding at the low affinity site. T19 is an interesting residue; in free MN4 the T19 imino is not observed due to line broadening. With the addition of one equivalent of cocaine this signal sharpens and appears as the most downfield peak in the imino region (18,21). With binding at the low affinity site, the T19 imino experiences line-broadening again and progressively reduces in intensity as the low affinity site is populated (Supplementary Figure S2). This phenomenon suggests that T19 occupies a position between both binding sites, as T19 is the most affected nucleotide upon binding at both the low- and high-affinity sites.

It is notable that cocaine binding at the high and low affinity sites produce a different effect on the imino NMR spectrum of MN4. Binding of the first cocaine ligand, at the high affinity site, results in the free and bound imino signals being in slow exchange on the NMR timescale with both free and singly-bound resonances visible (21). For binding at the low affinity site, the singly and doubly bound resonances are in fast exchange on the NMR timescale, with the

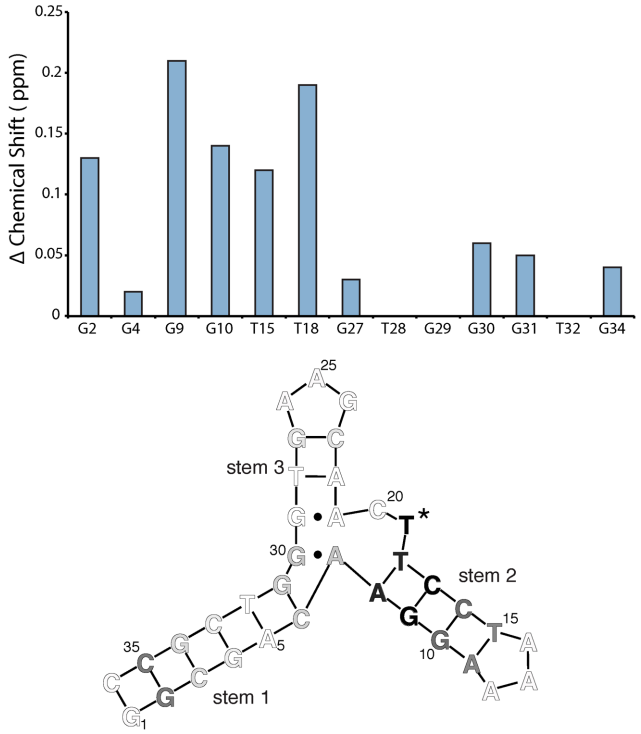

Figure 6. Changes in chemical shift with cocaine binding at the second binding site. (**Top**) Histogram showing the chemical shift perturbations ($\Delta\delta^1$H) of MN4 versus location in MN4. (**Bottom**) Chemical shift perturbations mapped onto the secondary structure of the cocaine aptamer. The residues that move most are shown in shades of gray, with the residues that shift the most shown in black and those that do not shift shown in white. T19, which line broadens into the baseline in the fully saturated complex, is also shown in black and indicated by an asterisk and not shown in the histogram due to it not being possible to calculate a $\Delta\delta$ for this residue.

population-weighted average chemical shift observed (Supplementary Figure S2). In order to push the two cocaine molecule–MN4 complex into a near fully-doubly-bound state a large (40-fold) excess of cocaine was required. This is best shown by the imino resonance of T19, where the signal is exchange broadened in the MN4•(cocaine)$_2$ sample and G9 and G10 which only fully finish shifting at a 40:1 molar excess (Supplementary Figure S2).

In order to test the reversibility of binding at the low affinity site, we took the 0 M NaCl NMR sample of MN4 with a 40-fold excess of cocaine and added NaCl to a final concentration of 200 mM (Figure 5). With the added NaCl, the effects on the NMR spectrum of binding at the low affinity site disappear and this sample is nearly identical to that of the 1:1 (MN4:cocaine) sample in 200 mM NaCl, as well as the 1:1 (MN4:cocaine) sample in 0 M NaCl. This shows that binding at the second site is completely reversible and depends on the amount of NaCl present in solution.

NMR-monitored titrations of MN4 with quinine were also performed (Supplementary Figure S4). As for the cocaine binding NMR experiments, two samples were prepared, one with no NaCl added and one with 200 mM NaCl. Both ligand-free MN4 samples looked essentially identical to each other and to the ligand-free samples used in the cocaine titrations (Figure 5; Supplementary Figure S4). Upon the addition of 1 equivalent of quinine we observe similar spectral changes in the NaCl free and 200 mM NaCl samples as we previously reported for MN4•(quinine) (18). Adding a 2.5-fold excess of quinine to the 200 mM NaCl sample resulted in no signals significantly changing their chemical shift though the signal intensity of T15 was reduced with quinine addition (Supplementary Figure S4). This lack of changes in the NMR signal in high salt with the addition of quinine past a 1:1 ratio is consistent with our ITC results that show no binding past one equivalent occurring in high salt conditions. For the NaCl-free sample, adding a 2.5-fold excess of quinine resulted in the disappearance of numerous signals in the NMR spectrum, but no new signals appeared. Presumably this is due to a number of signals in the low-affinity binding site being in intermediate exchange on the NMR timescale between the one and two-ligand bound states of MN4. Due to the low solubility of quinine compared with cocaine we were unable to add enough ligand to sufficiently saturate the two-ligand bound state to observe the 2:1 bound resonances. The signals that disappear with quinine addition past one equivalent include those of T15 and T18, both of these residues are in stem 2 on MN4 (Figure 1) and are among the nucleotides the most affected by cocaine binding at the low affinity site.

CONCLUSIONS

We have demonstrated using ITC and NMR spectroscopy that the cocaine-binding aptamer has the ability to bind two copies of its ligand at low NaCl concentrations. Both cocaine and quinine binding at the second site have a lower affinity than at the first site and increasing the concentration of NaCl can eliminate binding at the second site. Previous studies, by others and us, have looked at binding by the aptamer at relatively high NaCl concentrations and consequently binding at this second site was not previously observed. A benefit of this second binding site to biosensor design could be to extend the dynamic range of a cocaine sensor. By working at a low NaCl concentration the two sites with two different binding affinities should act in a similar fashion as using oligonucleotide inhibitors to alter the dynamic range of the cocaine-binding aptamer (33).

The ability to control ligand binding at the second site by adjusting the NaCl concentration is rare for aptamers. The only other example, known to us, is the neomycin B RNA aptamer that displayed NaCl-dependent binding at its two low affinity sites. However, aminoglycosides are known to frequently display non-specific RNA binding in addition to their interactions at a specific binding site (34,35). Aminoglycosides even interact with ATP in an electrostatic manner (36). What we demonstrate here is the first NaCl-controlled binding by an aptamer to ligands not known to bind nucleic acids nonspecifically. Other functional nucleic acid molecules, such as the ATP DNA aptamer (25,26) and the aptamer domain from the THF riboswitch (24) bind two copies of their ligands, but they have not been shown to have the ability to control the switch from single to two-sited binding by such a simple change as the buffer concentration of NaCl that we see here with the cocaine-binding aptamer. Considering the wide-spread usage of the cocaine-binding aptamer in biotechnology, the ability to control one

of two binding events by changing the NaCl concentration may prove useful in applications such as aptamer controlled cargo release (37) and aptamer based materials and sensing applications. This work also demonstrates that *in vitro* selected molecules can have as complex a function as those found in nature.

SUPPLEMENTARY DATA

Supplementary Data are available at NAR Online.

ACKNOWLEDGEMENTS

We thank members of the Johnson lab (York University, Toronto) for useful discussions, Howard Hunter (York University, Toronto) for help with NMR experiments and Robert Harkness, Lee Freiburger and Anthony Mittermaier (McGill University, Montreal) for useful discussions and for sharing their Matlab scripts.

FUNDING

Natural Sciences and Engineering Research Council of Canada (NSERC, grant number RGPIN-238562-2013) (to P.E.J.). Funding for open access charge: York University.
Conflict of interest statement. None declared.

REFERENCES

1. Breaker,R.R. (2002) Engineered allosteric ribozymes as biosensor components. *Curr. Opin. Biotechnol.*, **13**, 31–39.
2. Vinkenborg,J.L., Karnowski,N. and Famulok,M. (2011) Aptamers for allosteric regulation. *Nat. Chem. Biol.*, **7**, 519–527.
3. Stojanovic,M.N., de Prada,P. and Landry,D.W. (2000) Fluorescent sensors based on aptamer self-assembly. *J. Am. Chem. Soc.*, **122**, 11547–11548.
4. Stojanovic,M.N., de Prada,P. and Landry,D.W. (2001) Aptamer-based folding fluorescent sensor for cocaine. *J. Am. Chem. Soc.*, **123**, 4928–4931.
5. Stojanovic,M.N. and Landry,D.W. (2002) Aptamer-based colorimetric probe for cocaine. *J. Am. Chem. Soc.*, **124**, 9678–9679.
6. Baker,B.R., Lai,R.Y., Wood,M.S., Doctor,E.H., Heeger,A.J. and Plaxco,K.W. (2006) An electronic, aptamer-based small-molecule sensor for the rapid, label-free detection of cocaine in adulterated samples and biological fluids. *J. Am. Chem. Soc.*, **128**, 3138–3139.
7. Sachan,A., Ilgu,M., Kempema,A., Kraus,G. and Nilsen-Hamilton,M. (2016) Specificity and ligand affinities of the cocaine aptamer: impact of structural features and physiological NaCl. *Anal. Chem.*, **88**, 7715–7723.
8. Yu,H., Canoura,J., Guntupalli,B., Lou,X. and Xiao,Y. (2016) A cooperative-binding split aptamer assay for rapid, specific and ultra-sensative fluorescence detectoin of cocaine in saliva. *Chem Sci*, DOI: 10.1039/c6sc01833e.
9. Neves,M.A., Blaszykowski,C., Bokhari,S. and Thompson,M. (2015) Ultra-high frequency piezoelectric aptasensor for the label-free detection of cocaine. *Biosens. Bioelectron.*, **72**, 383–392.
10. Neves,M.A., Blaszykowski,C. and Thompson,M. (2016) Utilizing a key aptamer structure-switching mechanism for the ultrahigh frequency detection of cocaine. *Anal. Chem.*, **88**, 3098–3106.
11. Malile,B. and Chen,J.I. (2013) Morphology-based plasmonic nanoparticle sensors: controlling etching kinetics with target-responsive permeability gate. *J. Am. Chem. Soc.*, **135**, 16042–16045.
12. Das,J., Cederquist,K.B., Zaragoza,A.A., Lee,P.E., Sargent,E.H. and Kelley,S.O. (2012) An ultrasensitive universal detector based on neutralizer displacement. *Nature Chem.*, **4**, 642–648.
13. Sharma,A.K. and Heemstra,J.M. (2011) Small-molecule-dependent split aptamer ligation. *J. Am. Chem. Soc.*, **133**, 12426–12429.
14. Xiang,Y. and Lu,Y. (2011) Using personal glucose meters and functional DNA sensors to quantify a variety of analytical targets. *Nat. Chem.*, **3**, 697–703.
15. Freeman,R., Sharon,E., Teller,C. and Willner,I. (2010) Control of biocatalytic transformations by programmed DNA assemblies. *Chem. Eur. J.*, **16**, 3690–3698.
16. Shlyahovsky,B., Li,D., Weizmann,Y., Nowarski,R., Kotler,M. and Willner,I. (2007) Spotlighting of cocaine by an autonomous aptamer-based machine. *J. Am. Chem. Soc.*, **129**, 3814–3815.
17. Pei,R., Shen,A., Olah,M.J., Stefanovic,D., Worgall,T. and Stojanovic,M.N. (2009) High-resolution cross-reactive array for alkaloids. *Chem. Commun.*, 3193–3195.
18. Reinstein,O., Yoo,M., Han,C., Palmo,T., Beckham,S.A., Wilce,M.C.J. and Johnson,P.E. (2013) Quinine binding by the cocaine-binding aptamer. Thermodynamic and hydrodynamic analysis of high-affinity binding of an off-target ligand. *Biochemistry*, **52**, 8652–8662.
19. Slavkovic,S., Altunisik,M., Reinstein,O. and Johnson,P.E. (2015) Structure-affinity relationship of of the cocaine-binding aptamer with quinine derivatives. *Bioorg. Med. Chem.*, **23**, 2593–2597.
20. Harkness,R.W., Slavkovic,S., Johnson,P.E. and Mittermaier,A.K. (2016) Rapid characterization of folding and binding interactions with thermolabile ligands by DSC. *Chem. Commun.*, **52**, 13471–13474.
21. Neves,M.A.D., Reinstein,O. and Johnson,P.E. (2010) Defining a stem length-dependant binding mechanism for the cocaine-binding aptamer. A combined NMR and calorimetry study. *Biochemistry*, **49**, 8478–8487.
22. Reinstein,O., Neves,M.A.D., Saad,M., Boodram,S.N., Lombardo,S., Beckham,S.A., Brouwer,J., Audette,G.F., Groves,P., Wilce,M.C.J. *et al.* (2011) Engineering a structure switching mechanism into a steroid binding aptamer and hydrodynamic analysis of the ligand binding mechanism. *Biochemistry*, **50**, 9368–9376.
23. Neves,M.A.D., Reinstein,O., Saad,M. and Johnson,P.E. (2010) Defining the secondary structural requirements of a cocaine-binding aptamer by a thermodynamic and mutation study. *Biophys. Chem.*, **153**, 9–16.
24. Trausch,J.J., Ceres,P., Reyes,F.E. and Batey,R.T. (2011) The structure of a tetrahydrofolate-sensing riboswitch reveals two ligand binding sites in a single aptamer. *Structure*, **19**, 1413–1423.
25. Huizenga,D.E. and Szostak,J.W. (1995) A DNA aptamer that binds adenosine and ATP. *Biochemistry*, **34**, 656–665.
26. Lin,C.H. and Patel,D.J. (1997) Structural basis of DNA folding and recognition in an AMP-DNA aptamer complex: distinct architectures but common recognition motifs for DNA and RNA aptamers complexed to AMP. *Chem. Biol.*, **4**, 817–832.
27. Cowan,J.A., Ohyama,T., Wang,D. and Natarajan,K. (2000) Recognition of a cognate RNA aptamer by neomycin B: quantitative evaluation of hydrogen bonding and electrostatic interactions. *Nucleic Acids Res.*, **28**, 2935–2942.
28. Jose,A.M., Soukup,G.A. and Breaker,R.R. (2001) Cooperative binding of effectors by an allosteric ribozyme. *Nucleic Acids Res.*, **29**.
29. Freiburger,L.A., Auclair,K. and Mittermaier,A.K. (2009) Elucidating protein binding mechanisms by variable-c ITC. *ChemBioChem*, **10**, 2871–2873.
30. Piotto,M., Saudek,V. and Sklenar,V. (1992) Gradient-tailored excitation for single-quantum NMR spectroscopy of aqueous solutions. *J. Biomol. NMR*, **2**, 661–665.
31. Hwang,T.L. and Shaka,A.J. (1995) Water suppression that works. Excitation sculpting using arbitrary wave-forms and pulsed-field gradients. *J. Mag. Res. A*, **112**, 275–279.
32. Freire,E., Schon,A. and Velazquez-Campoy,A. (2009) Isothermal titration calorimetry: general formalism using binding polynomials. *Methods Enzymol.*, **455**, 127–155.
33. Porchetta,A., Vallee-Belisle,A., Plaxco,K.W. and Ricci,F. (2012) Using distal-site mutations and allosteric inhibition to tune, extend, and narrow the useful dynamic range of aptamer-based sensors. *J. Am. Chem. Soc.*, **134**, 20601–20604.
34. Verhelst,S.H., Michiels,P.J., van der Marel,G.A., van Boeckel,C.A. and van Boom,J.H. (2004) Surface plasmon resonance evaluation of various aminoglycoside-RNA hairpin interactions reveals low degree of selectivity. *ChemBioChem*, **5**, 937–942.
35. Tavares,T.J., Beribisky,A.V. and Johnson,P.E. (2009) Structure of the cytosine-cytosine mismatch in the thymidylate synthase mRNA

binding site and analysis of its interaction with the aminoglycoside paromomycin. *RNA*, **15**, 911–922.
36. Ohyama,T., Wang,D. and Cowan,J.A. (1998) Anion coordination by aminoglycosides: structural and charge effects. *Chem. Commun.*, 467–468.
37. Douglas,S.M., Bachelet,I. and Church,G.M. (2012) A logic gated nanorobot for targeted transport of molecular payloads. *Science*, **335**, 831–834.